Temperature and Crystallinity Profiles Generated in a Polycaprolactone/Starch Blend Under Different Cooling Conditions

R. A. RUSECKAITE,[1,2] P. M. STEFANI,[3] V. P. CYRAS,[1] J. M. KENNY,[4] A. VÁZQUEZ[1]

[1] Research Institute of Material Science and Technology, INTEMA, Mar del Plata University, Juan B. Justo 4302, 7600 Mar del Plata, Argentina

[2] Faculty of Sciences, Mar del Plata University, Funes 3350, 7600 Mar del Plata, Argentina

[3] Facultad Regional Concepción del Uruguay Universidad Tecnologica Nacional, Ing. Pereira 676, 3260 Concepción del Uruguay, Argentina

[4] Materials Department, Engineering Faculty, Perugia University, Loc. Pentima bassa 21, Terni, Italy

Received 9 October 2000; accepted 26 January 2001

ABSTRACT: This work concerns the numerical simulation of the temperature profiles and the degree of crystallinity through the thickness of a part made from a commercial biodegradable material based on caprolactone and starch (Mater-Bi Z), as a function of the cooling conditions from the melt. The crystallization kinetics during cooling conditions was evaluated experimentally by calorimetry and the Kamal–Chu equation was used to describe the degree of crystallinity developed during constant cooling rate experiments. This equation coupled with the thermal energy equation, through a heat source term, described the heat generated during crystallization of the polymer. The numerical solution of the system of differential equations was obtained using an implicit finite-difference method. © 2001 John Wiley & Sons, Inc. J Appl Polym Sci 82: 3275–3283, 2001

Key words: crystallization; polycaprolactone; starch

INTRODUCTION

The behavior of semicrystalline polymers during nonisothermal crystallization from the molten state is of increasing technological importance because these conditions are the closest to real industrial processing conditions. In fact, during fabrication the polymeric material is subjected to one or more cycles of heating, melting, cooling, and solidification of polymer melts that determine the morphology and final properties of the product. The degree of crystallinity and morphology developed in the matrix may be significantly influenced by the rate at which the part is cooled from the melt. Cooling a thick part too rapidly produces temperature gradients through the thickness of the part, which may subsequently lead to crystallinity and morphology gradients. These gradients may lead to undesirable variations in the me-

Correspondence to: A. Vázquez (anvazque@fi.mdp.edu.ar).
Contract grant sponsor: Fundacion Antorchas (Argentina).
Contract grant sponsor: National Research Council (CONICET).

chanical properties of the part.[1] In recent years, efforts have been devoted to the engineering analysis or mathematical simulation of processes such as extrusion, blow molding, and injection molding.[2–5] Most of these treatments have involved solving the standard transport equation with appropriate boundary and initial conditions coupled to the isothermal macrokinetic approach of the Avrami equation[6] or its modifications, which account for nonisothermal conditions such as the empirical equation of Kamal and Chu,[7] Nakamura,[8] or Ozawa.[9]

Mater-Bi Z is a new class of semicrystalline polymeric material based on polycaprolactone (PCL) and starch (S).[10] Nowadays, this material is receiving increasing industrial attention for use as a commodity plastic, not only because of its biodegradablility and compatibility with various forms of waste disposal but also because of its wide range of processing grades.[11–13] Recently, Cyras et al.[14] reported the study of the isothermal and nonisothermal crystallization kinetics of caprolactone/starch and caprolactone/starch composite with sisal fiber. However (and to the best of our knowledge), there is no study reported in the literature concerning mathematical simulation of processes such as molding applied to the caprolactone/starch blend.

The aim of this work is to develop a model to describe the degree of crystallinity and temperature profiles developed through the thickness of a part of caprolactone/starch blend as a function of the cooling conditions from the melt. The Kamal–Chu model will be used to predict the kinetic parameters for the nonisothermal crystallization.

EXPERIMENTAL

Mater-Bi Z was provided by Novamont (Italy); its starch and natural additive content was higher than 40% w/w.[11] The nonisothermal crystallization kinetic was measured by calorimetric analysis using a differential scanning calorimeter (DSC) Mettler 30, operating from −50°C to 350°C under nitrogen atmosphere. The samples were first heated from room temperature to 80°C, at a heating rate of 10°C/min. The samples were maintained at 80°C for 10 min, after which they were cooled at different cooling rates (0.083, 0.166, 0.33, and 0.5 by K/s). The relative degree of crystallinity X_r was obtained as a function of the crystallization temperature as

$$X_r = \frac{\int_{T_0}^{T} \left(\frac{dH_c}{dT}\right) dT}{\int_{T_0}^{T_\infty} \left(\frac{dH_c}{dT}\right) dT} \quad (1)$$

where T_0 and T_∞ represent the onset and the end of crystallization temperatures, respectively.

Procedure

Nonisothermal Kinetic Model

Isothermal crystallization of semicrystalline polymers can be represented by the Avrami equation[6]:

$$X_r(t) = 1 - \exp(-kt^n) \quad (2)$$

where X_r is the relative degree of crystallinity; n is a mechanism constant, the value of which depends on the type of nucleation and growth-process parameters; and k is a composite rate constant involving both nucleation and growth-rate parameters.

This model can be applied only to crystal growth after nucleation. In fact, heterogeneous and homogeneous nucleation are thermally activated phenomena and their effects can be macroscopically detected by isothermal DSC experiments where the exothermal signal can be observed only after a delay (induction time), attributed to the formation of nuclei of critical size.[15] The induction time cannot be directly obtained from nonisothermal experiments, although it plays a fundamental role in determining the onset time for the crystal growth.

The nonisothermal crystallization can be approached by a differential model with a temperature-dependent kinetic constant like the empirical expression of Kamal and Chu[7]:

$$\frac{dX_r}{dt} = nk(T)(1 - X_r)t^{n-1} \quad (3)$$

An Arrenhius type of equation was used to represent the dependence of k with the temperature:

$$k = k_0 \exp\left[\frac{-E_a}{R(T_m^0 - T)}\right] \quad (4)$$

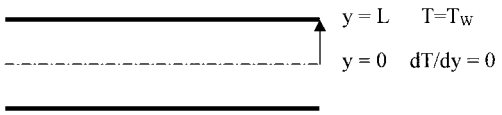

Figure 1 Mold configuration in the molding processing.

where E_a is the crystallization activation energy, k_0 is the preexponential constant, T_m^0 is the theoretical melting temperature, and R is the gas constant.

This model can be reduced to the classical Avrami equation in isothermal conditions.

The initial condition in a nonisothermal simulation is given by the induction time calculated as the sum of the contributions of isothermal steps evaluated from the isothermal crystallization experiments performed by DSC. The dependency of the isothermal induction time on temperature can be expressed as

$$t_i = k_{i0}\exp\left[\frac{E_i}{R(T_m^0 - T)}\right] \tag{5}$$

where k_{i0} is a preexponential factor and E_i is the activation energy for the nucleation process. The nonisothermal induction time (t_{ni}) is then computed by using a dimensionless parameter Q:

$$Q = \int_0^{t_{ni}} \frac{dt^*}{t_i} \tag{6}$$

where t_i is the isothermal induction time given by eq. (5). Numerical integration of eq. (6) is performed by taking $t^* = 0$ at the melting temperature (T_{m0}). The value $t^* = t_{ni}$ at which Q reaches unity represents the nonisothermal induction time.[15]

A nonlinear regression analysis based on the method of Marquardt[16] was used to find the best-fitting parameters to eqs. (3) and (4). The theoretical melting temperature (T_m^0), activation energy (E_i), and preexponential constant for the induction (k_{i0}) were taken from the literature.[14]

Formulation of the Simulation

Figure 1 represents a description of the mold configuration. The one-dimensional non-steady-state heat transfer through the mold thickness shown in Figure 1 is given by the following thermal energy equation:

$$\rho C_p \frac{\partial T}{\partial t} = k \frac{\partial T^2}{\partial y^2} + (-\Delta H)\frac{dX_r}{dt} \tag{7}$$

This equation relates the relative degree of crystallinity (X_r) and temperature (T) as functions of time (t) and the position in the mold thickness (y) for given values of crystallization heat (ΔH_c), thermal conductivity (k), density (ρ), and specific heat (C_p). The last term in eq. (7) is the heat source term associated with the heat generated during crystallization .

Equation (7) can be written as

$$\frac{\partial T}{\partial t} = \alpha \frac{\partial^2 T}{\partial y^2} + \frac{(-\Delta H_c)}{C_p}\frac{dX_r}{dt} \tag{8}$$

where $\alpha = k/\rho C_p$ is the thermal diffusivity.

The boundary conditions are the following:

$$y = 0 \quad dT/dy = 0 \tag{9}$$

$$y = L \quad T = T_w(t) = T_0 + qt \tag{10}$$

where q is the cooling rate and T_0 is the initial temperature.

The initial conditions are

$$T = T_0, \quad X_r = 0 \quad \text{at} \quad t = 0 \quad \forall y \tag{11}$$

The dimensionless form of the thermal energy may be written as

$$\frac{\partial \theta}{\partial \lambda} = \frac{\partial^2 \theta}{\partial \xi^2} + \beta \frac{dX_r}{d\lambda} \tag{12}$$

where

$$\theta = T/T_0 \quad \lambda = t\alpha/L^2 \quad \xi = y/L \quad \beta = \Delta H/C_p T_0 \tag{13}$$

The left-hand side of eq. (9) represents the change in the temperature with time. The first term on the right-hand side represents the heat transfer, attributed to conduction, and the second represents the heat generated, attributed to the phase change.

The thermal conductivity, the density, and the specific heat were assumed to be independent of

Table I Physical Constants Used in the Simulation

Thermal conductivity, κ	0.07	$J/s^{-1}/m^{-1}/K^{-1}$
Specific heat, C_p	1348.5	$J/K^{-1}/kg^{-1}$
Density, ρ	1230.8	kg/m^3
Crystallization heat, ΔH_c	29530	J/kg
Equilibrium melting temperature, T_m^0	339	K
Initial temperature, T_0	353	K
Activation energy nonisothermal crystallization, E_a	1954	J/mol
Kinetic exponent, n	2.23	
Preexponential constant, k	0.85058	s^{-n}
Activation energy isothermal induction time, E_i	2361	J/mol
Preexponential constant isothermal induction time, k_{i0}	4.7367×10^{-4}	s^{-1}

temperature, although this is not really necessary.[17]

The density of the caprolactone/starch blend was calculated as mixture rule:

$$\rho = V_{\mathrm{PCL}}\rho_{\mathrm{PCL}} + V_{\mathrm{starch}}\rho_{\mathrm{starch}} \tag{14}$$

where ρ_{PCL} is the density of the PCL, ρ_{starch} is the density of the starch,[18,19] and V_{PCL} and V_{starch} are the volume content of PCL and starch, respectively.

The thermal conductivity was calculated by combining the thermal conductivities of both components, using the parallel model:

$$\frac{1}{k} = \frac{V_{\mathrm{PCL}}}{k_{\mathrm{PCL}}} + \frac{V_{\mathrm{starch}}}{k_{\mathrm{starch}}} \tag{15}$$

where k_{PCL} and k_{starch} are the individual thermal conductivities taken from the literature.[20,21]

The specific heat capacity was calculated as

$$C_p = w_{\mathrm{PCL}}C_{p\ \mathrm{PCL}} + w_{\mathrm{starch}}C_{p\ \mathrm{starch}} \tag{16}$$

where $C_{p\ \mathrm{PCL}}$ is the specific heat capacity of the PCL, $C_{p\ \mathrm{starch}}$ is the specific heat capacity of the starch,[18,20] and w_{PCL} and w_{starch} are the weight content of PCL and starch, respectively. Table I shows the parameters used in the dimensionless thermal energy equation.

RESULTS AND DISCUSSION

The crystallization exotherms at various cooling rates are represented in Figure 2. The exothermic peak temperature (T_p) shifts to lower temperatures as the cooling rate increases. The same behavior was observed for the melt crystallization of poly(hydroxybutyrate)[22] and nylon 11.[23] The values of T_p and the relative degree of crystallinity at T_p are shown in Table II. Crystallization enthalpies were almost not affected by the cooling conditions; thus, a mean value was used, at least for the simulation (Table I).

Integration of exothermic peaks during nonisothermal conditions give the relative degree of crystallinity as a function of the temperature. To obtain kinetic information, the experimental relative crystallization data collected over a wide range of cooling rates (0.083, 0.166, 0.33, and 0.5 K/s) were fitted to the Kamal–Chu differential model , using a nonlinear multivariable regression method.[16] The predicted kinetic parameters obtained with the best fit were: the Avrami exponent $n = 2.234$; the crystallization activation energy $E_a = 1954$ J/mol; and the preexponential factor $k_0 = 0.85058\ s^{-2.234}$. Figure 3 shows the comparison between experimental data and predicted curves. The model fits well for X_r values ranging from 0 to 0.80 and shows a good performance for low cooling rates. Recently, one approach used in the literature to describe the nonisothermal crystallization process of caprolactone/starch blend consists of applying the integral expression of Nakamura[8] (which extends the general Avrami theory to nonisothermal conditions), using the kinetic parameters obtained from the analysis of the isothermal data.[14] It must be taken into account that in nonisothermal crystallization, the values of k and n do not have the same physical significance as in isothermal crystallization because, under nonisothermal conditions, the temperature changes constantly. However, this approach has the ability of describing experimental data with a moderate mismatch.

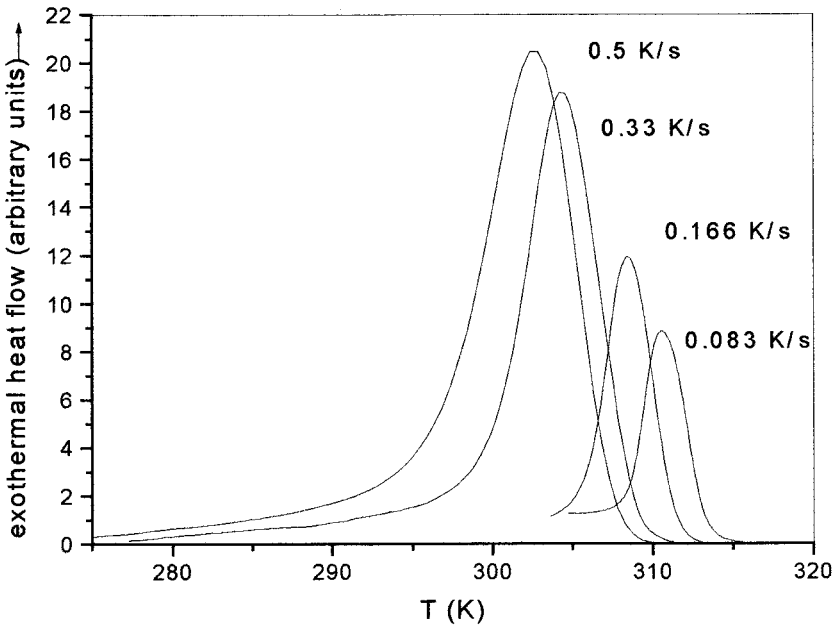

Figure 2 Crystallization exotherms during nonisothermal crystallization of caprolactone/starch blend at different cooling rates.

The analytical procedure used in this work automatically provides a single set of kinetic parameters for different cooling rates; thus, these parameters can be easily used in modeling actual processing conditions.

The temperature, crystallization rate, and relative degree of crystallinity profiles developed under different cooling conditions applied to the wall of a caprolactone/starch blend–molded part were calculated by solving the thermal energy equation [eq. (12)] coupled to the nonisothermal crystallization model [eqs. (3)–(6)]. An implicit finite-difference method (Crank–Nicholson scheme) was used to solve the thermal energy equation. The dX_r/dt in the heat source term of eq. (12) was evaluated by using an explicit method. The sample thickness (from 1 to 10 mm) was divided in 10 evenly spaced nodes between the centerline and the wall. The time step at which the system was solved was less than 0.0024 s. Cooling rates used in the simulation were 0.083, 0.166, 0.33, and 0.5 K/s, and were similar to those reported in the literature for predicting the evolution of temperature and crystallinity during the cooling of a part of a semicrystalline polymer reinforced with carbon fiber.[1]

Table II Parameters of the Mater-Bi Z™ Nonisothermal Crystallization Process

Cooling Rate (K/s)	T_p (K)	X_r
0.083	310.5	0.48
0.166	308.4	0.49
0.33	304.2	0.42
0.5	302.8	0.33

The temperature curves at evenly spaced points along the horizontal axis of symmetry of the simulation domain for a thickness of 4 mm at a cooling rate of 0.166 K/s are plotted in Figure 4. During cooling, three steps can be distinguished:

1. Cooling of the piece from the molten state, before the beginning of crystallization. In this stage, the temperature profiles respond to Fourier's law under nonsteady conditions, which is a function of the conductivity of the melt, the thickness of the part, and the cooling rate.
2. During crystallization, the temperature profiles generated are the result of two competing factors: (a) the rate of heat generated by the exothermic crystallization reaction and (b) the conductive heat flux toward the walls. As the crystallization begins, an increment in temperature occurs.

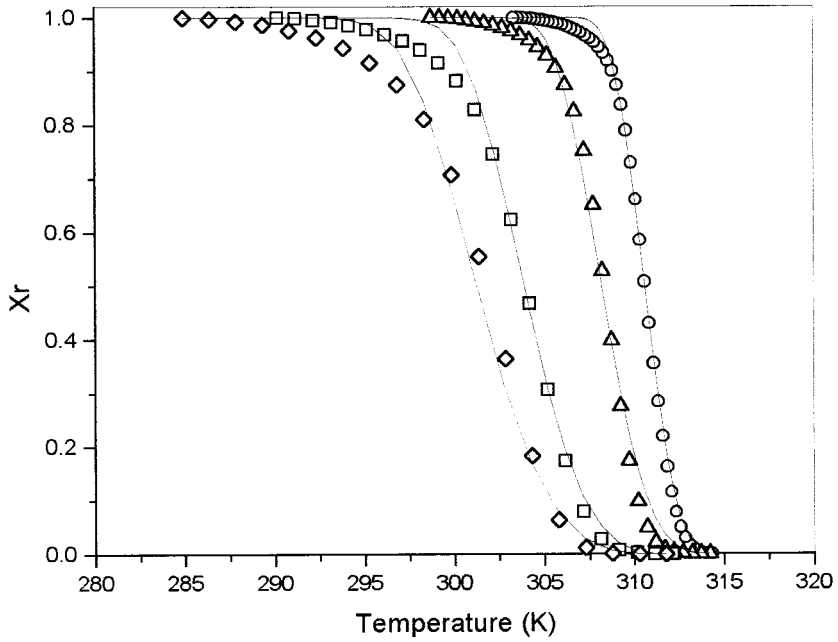

Figure 3 Relative degree of crystallization versus temperature during nonisothermal crystallization. Points are experimental data at 0.083 K/s (○), 0.166 K/s (△), 0.333 K/s (□), and 0.5 K/s (◇). The solid lines are the Kamal–Chu model predictions.

For positions deeper in the sample the model predicts an increase in the temperature profile because the heat generated during crystallization is higher than the rate of the conductive heat flux toward the walls. This effect is more pronounced as

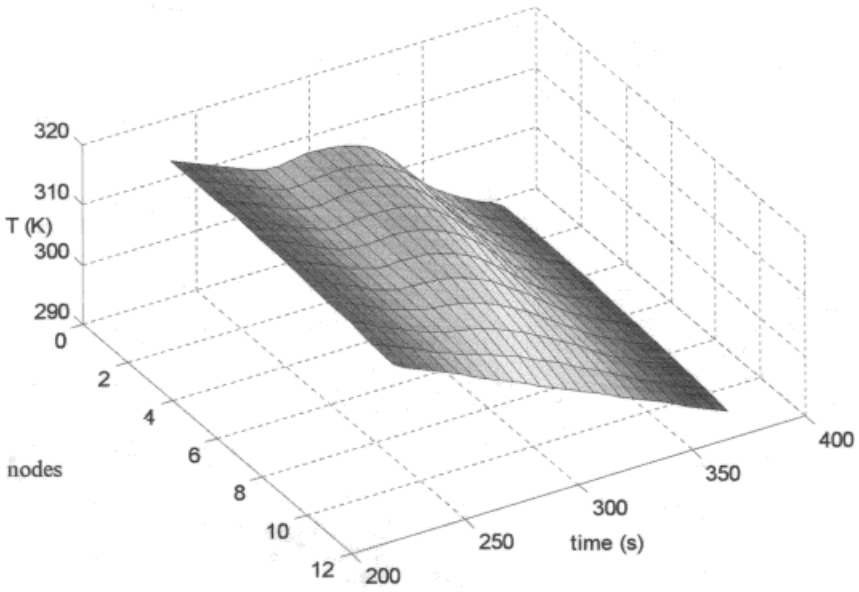

Figure 4 Cooling curves for different positions along the horizontal axis of symmetry of a piece 2 mm thick and at a cooling rate of 0.166 K/s. The first curve on the left corresponds to the mold wall and the last curve corresponds to the center of the piece ($L/2$).

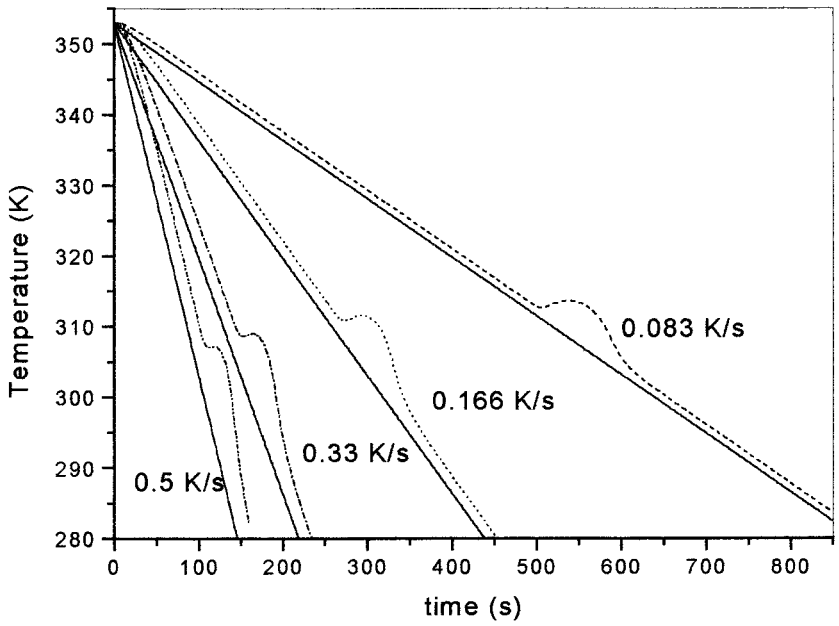

Figure 5 Effect of the different cooling rates on temperature profiles at the center of a piece 4 mm thick.

either the thickness of the part or the cooling rate increases.

3. Cooling a solid after crystallization, which is controlled by Fourier's law, but in this stage is a function of the conductivity of the solid.

These temperature gradients may lead to crystallinity and morphology gradients that may produce undesirable variations in mechanical properties of the part. Therefore, the model was used to predict the effect of the cooling conditions and part thickness on the temperature, crystallization rate, and degree of crystallinity profiles generated during molding.

Figure 5 shows the effect of the cooling rate on the temperature profile at the center of a piece 4 mm thick. The surface-to-center temperature gradient increases as the cooling rate increases. The model predicts that the crystallization begins at lower temperatures in the center as the cooling rate increases, in agreement with the calorimetric data. The same effect was found as the thickness increases, as shown in Figure 6. As a result, the higher the cooling rate or the thickness, the higher the temperature gradient at the center of the piece. These temperature gradients may lead to variations in the crystallization rate and crystallinity gradients within the part. Figure 7 represents the predicted crystallization rate and temperature gradients for two specific positions of a 4-mm-thick part. In the wall, the maximum crystallization rate occurred at about 275 s and no exothermic peak is observed as a consequence of the boundary condition imposed, whereas in the core region, temperature shows a maximum and a period of about 340 s was needed to complete crystallization. The shoulder observed in the crystallization rate curve, corresponding to the core region at about 280 s, can be associated with the increase in temperature during cooling. However, for a piece 2 mm thick, the model predicts no variations from the surface to the center, for all practical purposes, under all the cooling conditions analyzed. Indeed, the surface-to-center temperature gradient at 0.5 K/s was less than 1°C, so the crystallizations at the wall and in the core region are almost simultaneous at the maximum cooling rate analyzed. The surface-to-center crystallinity gradients become more pronounced as either the thickness or the cooling rate increases. For cooling rates higher than 0.166 K/s, the model predicts no crystallization of the inner part (within the time scale considered) for pieces with thicknesses greater than 4 mm. Thus, cooling at a constant cooling rate may be applied only to pieces with thicknesses of 2 mm or less, thereby introducing minor crystallinity gradients.

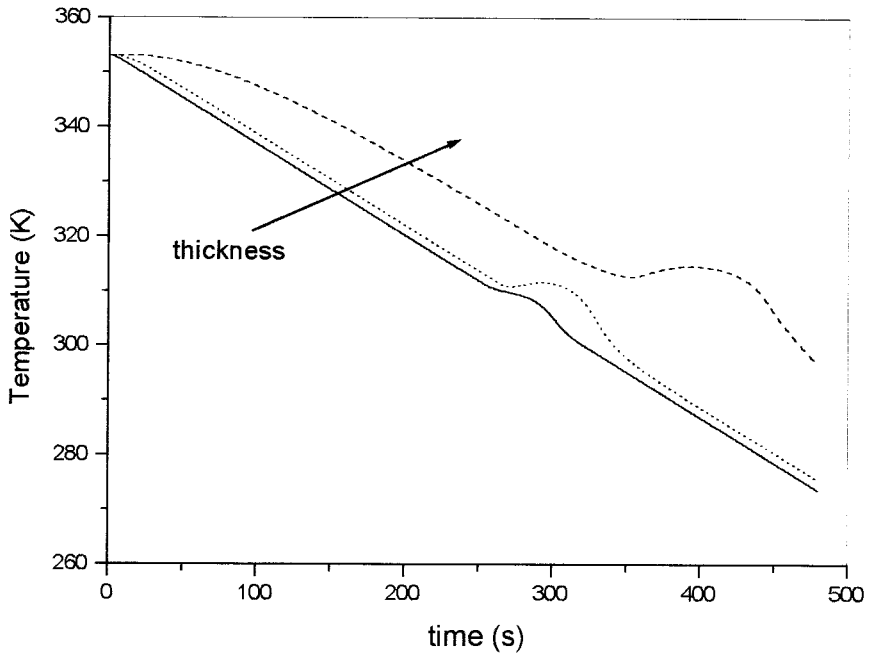

Figure 6 Effect of the part thickness on the temperature profiles at a cooling rate of 0.166°C/s.

To reproduce another processing condition, the model was then used to predict the evolution of temperature and crystallinity within a part of caprolactone/starch blend and under cooling at different constant temperatures. The wall temperatures evaluated were 293, 303, and 313 K for thicknesses varying from 1 to 10 mm. Figure 8 shows the cooling curves for different positions along the horizontal axis. The distance between two consecutive sampling points is 0.2 mm. Near the center the thermal gradient is low; hence, the rate of heat removal from the solidification front is small. As a consequence an increment in temperature is observed at a y-value of 1.2 mm, from 27 s to the end of the process. The crystallization heat produces a decrease in the crystallization rate, which is more pronounced in center. It is important to note that the heat generation term becomes more significant as the thickness and the wall temperature increase. As a consequence a surface-to-center delay in crystallization is observed. The model predicts paired crystallinity gradients for thicknesses less than 2 mm, by cooling at a constant cooling rate or at a constant wall temperature.

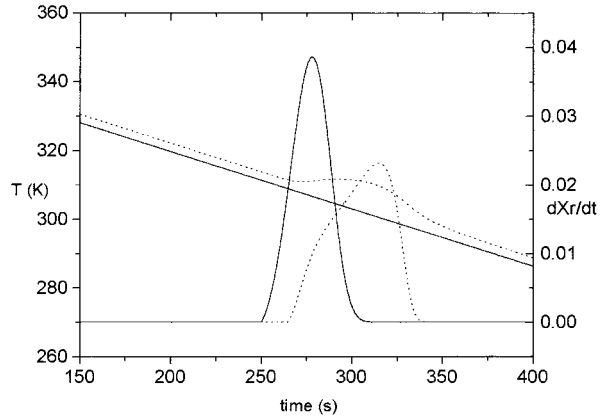

Figure 7 Effect of the thickness on the crystallization rate and temperature variation for two positions, the wall (—) and the center (· · ·), for a thickness of 4 mm and a cooling rate of 0.166 K/s: 2 mm (—), 4 mm (· · ·), and 10 mm (—).

CONCLUSIONS

The numerical simulation of molding a part of caprolactone/starch blend leads to the prediction of temperature, relative degree of crystallinity, and crystallization rate profiles generated under different cooling conditions applied to the wall: constant cooling rate and constant temperature. The model predicts paired crystallinity profiles

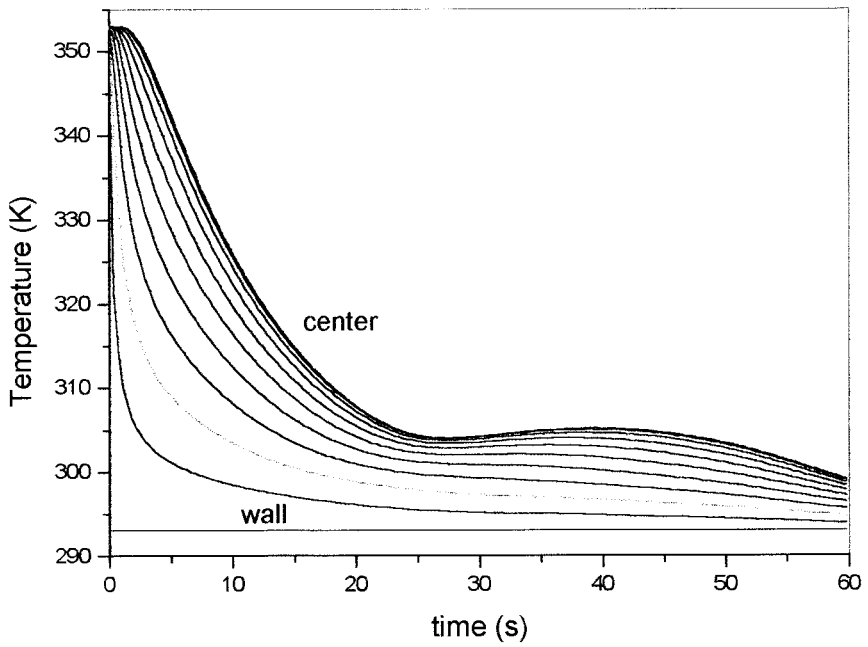

Figure 8 Cooling curves for different positions along the horizontal axis of a 4-mm-thick part cooling at 20°C.

for thicknesses less than 2 mm for both processing conditions. In this case, good mechanical and physical properties in the part are expected.

The authors acknowledge the financial support of Fundacion Antorchas (Argentina) and the National Research Council (CONICET).

REFERENCES

1. Deporter, J. K.; Baird, D. G. Polym Compos 1996, 17, 210.
2. Woo, A. W.; Wong, P.; Tang, Y.; Triacca, V.; Gloor, P.; Hrymak, A.; Hamielec, A. Polym Eng Sci 1995, 35, 151.
3. Chiu, W.-Y.; Chen, L.-W.; Wang, C.; Wang, D.-C. J Appl Polym Sci 1991, 43, 39.
4. Lee, W.; Springer, G. J Comp Mater 1987, 21, 1017.
5. Velisaris, C.; Seferis, J. Polym Eng Sci 1986, 28, 583.
6. Wunderlich, B. Macromolecular Physics, Vol. 2; Academic Press: New York, 1977.
7. Kamal, M.; Chu, E. Polym Eng Sci 1983, 23, 27.
8. Nakamura, K.; Katayama, K.; Amano, T. J Appl Polym Sci 1973, 17, 1031.
9. Ozawa, T. Polymer 1971, 12, 150.
10. Bastioli, C.; Bellotti, V.; Montino, A.; Tredici, G.; Lombi, R.; Ponti, R. U.S. Pat. 5,412,005, 1995.
11. Bastioli, C.; Bellotti, V.; Del Giudice, L.; Gilli, G.; in Biodegradable Polymers and Plastics; Vert, M.; Feijen, J.; Albertsson, A.-C.; Scott, G.; Chiellini, E., Eds.; Royal Society of Chemistry: Cambridge, UK, 1992.
12. Bastioli, C.; Degli Innocenti, E.; Guanella, I.; Romano, G. in Degradable Polymers, Recycling and Plastics Waste Management; Albertsson, A.-C.; Huang, S., Eds.; Marcel Decker: New York, 1995.
13. Solaro, R.; Corti, A.; Chiellini, E. J Environ Polym Degrad 1998, 4, 203.
14. Cyras, V. P.; Iannace, S.; Kenny, J. M.; Vázquez, A. Polym Compos to appear.
15. Torre, L.; Maffezzoli, A.; Kenny, J. J Appl Polym Sci 1995, 56, 985.
16. Marquardt, W. SIAM J 1963, 11, 431.
17. Warbington, R. H.; Crowe, W. C.; Seferis, J. C.; deVries, A. J.; Gehreke, R.; Zachmann, H. G. Colloid Polym Sci 1986, 264, 683.
18. Agari, Y.; Ueda, A. J Polym Sci Part B Polym Phys 1994, 32, 56.
19. Helman, D.; Lund, D., Eds. Handbook of Food Engineering; Marcel Dekker: New York, 1992.
20. Brandrup, J.; Immergut, E., Eds. Polymer Handbook, 2nd ed.; Wiley: New York, 1975.
21. Rahman, S., Ed. Food Properties Handbook; CRC Press: Boca Raton, FL, 1995.
22. An, Y.; Dong, L.; Mo, Z.; Liu, T.; Feng, Z. J Polym Sci Part B Polym Phys 1998, 36, 1305.
23. Liu, S.; Yu, Y.; Cui, Y.; Zhang, H.; Mo, Z. J Appl Polym Sci 1998, 70, 2371.